

Computer Simulation of a “Green Chemistry” Room-Temperature Ionic Solvent

C. J. Margulis, H. A. Stern,[†] and B. J. Berne*

Department of Chemistry, Columbia University, 3000 Broadway, New York City, New York 10027

Received: June 12, 2002

In the interests of making chemistry more environmentally friendly, room-temperature ionic liquids are currently being investigated as alternative solvents in industry and academia. In this paper, we present molecular dynamics simulations of 1-butyl-3 methylimidazolium hexafluorophosphate ([bmim][PF₆]). We compute radial distribution functions, average density, and mean-square displacements for the individual ions. With this information, diffusion coefficients are calculated and conductivities are estimated using the Nernst–Einstein relation. The time history of the mean-square displacement of the ions appears to indicate that the system exhibits complex dynamics with at least two different time scales for diffusion. We model this behavior using a generalized Langevin approach. Results compare well with experimental data reported in the literature.

1. Introduction

Ionic liquids that are air- and water-stable at ambient temperature have been the focus of extensive research in the past few years.¹ A reaction medium that is clean, recyclable, and a good solvent for both organic and inorganic compounds is appealing. These liquids do not evaporate and have high electrical conductivity and a wide electrochemical window. They also have excellent thermal and chemical stability and tolerance to strong acids. They are immiscible with a number of organic solvents and can be used as an alternative to water for systems with more than one phase. The fact that these liquids usually consist of bulky ionic organic molecules makes them ideal as solvents; they are highly polar and yet very poor coordinating solvents. The hope is that soon some of these solvents will replace damaging or toxic chemicals which are usually very volatile and/or difficult to recycle.

An excellent review article by Welton¹ describes many organic reactions that have successfully been performed with high yields using these liquids as solvents. In his review article, Welton also describes preparation and handling techniques. Physical and chemical properties of some of these solvents have only recently been investigated experimentally^{1–10} and theoretically.^{11–13}

Recently, Holbrey and co-workers² performed NMR and IR spectroscopy, polarizing optical microscopy, and differential scanning calorimetry of some of these ionic organic compounds. Noda and co-workers³ measured H and F NMR spectra and were able to determine ionic diffusion coefficients, viscosity, and ionic conductivities. As far as we know, the X-ray crystal structure is available only for a few compounds.^{4,5} UV–vis, IR^{6,7} spectra, and thermal properties⁸ are available for some of these salts as well. Despite this, physical and chemical data for most compounds of interest is still incomplete, and in general, it is difficult to find those for which X-ray structure, UV, IR, diffusion constants, conductivity, and melting point are known.

From a theoretical point of view, one would like to know how an ionic liquid is different at the molecular level from common organic solvents such as tetrahydrofuran or methanol. How structured is it? How correlated is the motion of the ions?

Are these liquids similar to glasses or inorganic molten salts? Do they diffuse independently, or is there strong ion association? In this paper, we investigate structural and dynamical properties for 1-butyl-3 methylimidazolium hexafluorophosphate ([bmim]-[PF₆]), which is depicted in Figure 1. This particular compound was chosen as it appears to be the ionic solvent for which the widest range of physicochemical properties has been characterized experimentally.

2. Methods

We performed classical molecular dynamics simulations using a potential energy function of the form

$$U = U_{\text{stretch}} + U_{\text{bend}} + U_{\text{torsion}} + U_{\text{LJ}} + U_{\text{Coulomb}}, \quad (1)$$

where

$$U_{\text{stretch}} = \sum_{\text{bonds}} K_r (r - r_{\text{eq}})^2 \quad (2)$$

$$U_{\text{bend}} = \sum_{\text{angles}} K_\theta (\theta - \theta_{\text{eq}})^2 \quad (3)$$

$$U_{\text{torsion}} = \sum_{\text{dihedrals}} \sum_{i=1}^3 V_i [1 + \cos(\phi + f_i)] \quad (4)$$

$$U_{\text{LJ}} = \sum_{i < j} 4\epsilon_{ij} [(\sigma_{ij}/r_{ij})^{12} - (\sigma_{ij}/r_{ij})^6] \quad (5)$$

$$U_{\text{Coulomb}} = \sum_{i < j} q_i q_j / r_{ij} \quad (6)$$

In the case of [bmim], parameters for the stretch, bend, torsion, and Lennard-Jones terms were taken from the OPLS/AA force field,¹⁴ whereas partial charges q_i were taken from fits to the electrostatic potential (ESP) computed from ab initio calculations at the Hartree–Fock level, with 6-31G** basis set performed with the Jaguar¹⁵ package. Charges on equivalent hydrogens were averaged to obtain the same single value. Parameters for [PF₆] were obtained from the work of Kaminski et al.¹⁶ A table of all parameters used is available as Supporting Information.

The system simulated consisted of 256 pairs of ions, making a total of 8192 atoms. Periodic boundary conditions were

* To whom correspondence should be addressed.

[†] Currently at Cornell University.

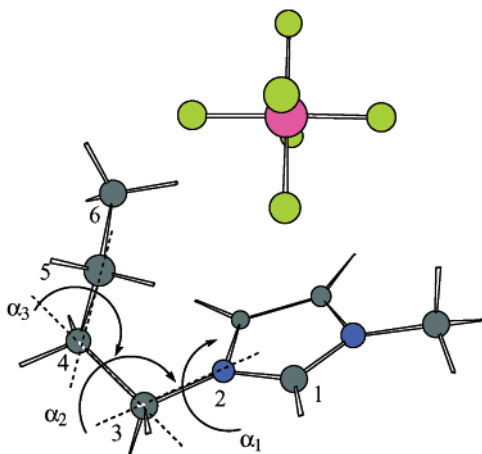


Figure 1. Snapshot of the molecular system (1-butyl-3-methylimidazolium hexafluorophosphate) used in our calculations. Atoms 1–4, 2–5, and 3–6 define dihedral angles α_1 , α_2 , and α_3 respectively.

employed using the particle–particle particle-mesh Ewald method^{17,18} to treat the long-range electrostatic interactions. The reference system propagator algorithm (r-RESPA)^{19,20,17} was employed with a time step of 0.5 fs for the fast, short-range intramolecular forces, and 2 fs for the slower, long-range degrees of freedom. Constant temperature and pressure (*NPT*) simulations were performed with Nosé–Hoover chain (NHC) thermostats and an Andersen–Hoover-type barostat.^{21,22} The calculations were performed using the program SIM developed in the Berne group.²³

The system was first equilibrated at constant temperature (303 K) and pressure (1 atm) for at least 200 ps until the density was equilibrated. To make sure the system was not getting trapped in a glassy state, several simulations starting from very different initial conditions were performed. Some of these initial conditions were lattices; others consisted of ions randomly placed and oriented. In all cases, initial conditions were chosen to have very low initial density. All simulations converged to the same average density and yielded nearly identical radial distribution functions.

In our set of production runs, 20 independent constant energy and volume simulations of 50 ps each were performed starting from equilibrated initial conditions. An equal number of simulations were performed at constant volume and temperature for the computation of radial distribution functions.

3. Results and Discussion

Experimental measurements of room temperature (291–303 K) densities reported in the literature for ionic liquids range from 1.1 to 1.6 g/cm³.⁹ In particular, Suarez and co-workers¹⁰ reported a value of 1.37 g/cm³ for the density of [bmim][PF₆] at 303 K. Our constant temperature and pressure results at the same temperature yielded an average of density of 1.31 g/cm³. Figure 2 parts a and c display the mean-square displacement as a function of time for the centers of mass of [bmim] and [PF₆], respectively. If one compares Figure 2 with the behavior of the mean-square displacement of room-temperature water²⁴ or even that of inorganic molten salts,²⁵ it appears that the dynamics of an ionic organic liquid are more complex. In Figure 2 parts a and c, one observes three different time scales: a fast process on a time scale of about three or four picoseconds, then a nonlinear intermediate regime, and finally diffusive linear behavior. It is worth noting that the first process is not simple ballistic motion. (The quadratic time dependency indicating ballistic motion occurs at time zero and lasts for only femto-

seconds.) Rather, the time dependency is more complicated than quadratic and most likely indicates the exploration of a local basin. The intermediate regime is probably associated with basin hopping. Only after about 15 ps can the linear dependence associated with simple diffusion be observed. These results seem consistent with those obtained by Hanke¹¹ and co-workers in their simulations of similar compounds using a different force field.

This type of behavior is characteristic of mildly supercooled water²⁶ and of vacancy migration in some ionic crystals.²⁷ Most room-temperature organic ionic liquids are barely above their melting point; in most cases, they also display glass transitions at about room temperature. Hence, it is not surprising that the mean square displacement as a function of time might look like that of supercooled liquids. In fact, if we plot time in a logarithmic scale, see Figure 3, the plots look very similar to those of supercooled water reported by Gallo and co-workers.²⁶ Overlaid in Figure 2 parts a and c is the best linear fit in the range 20–40 ps corresponding to the aforementioned linear regime. From the slope of this line and the Einstein relation $2Dt = \frac{1}{3}\langle |r_i(t) - r_i(0)|^2 \rangle$, we obtain diffusion constants of 1.43×10^{-11} and 1.28×10^{-11} m²/s for [bmim] and [PF₆], respectively. These results are comparable to those reported by Noda and co-workers from their NMR measurements on slightly different compounds.³

One can model the dependency of the mean square displacement with time using a generalized Langevin approach.²⁸ If one assumes the friction kernel is the sum of a fast and a slow term, corresponding respectively to a “fast” exploration of local energy basins and a “slow” escape from one energy basin into another energy basin, one can write the following expression for the normalized velocity correlation function:

$$\frac{\partial C(t)}{\partial t} = - \int_0^t d\tau [K_f(\tau) + K_s(\tau)] C(t - \tau) \quad (7)$$

where

$$C(t) = \frac{\langle \mathbf{v}(t) \cdot \mathbf{v}(0) \rangle}{\langle v^2 \rangle} \quad (8)$$

The simplest approach involves defining the fast and slow components of the kernel in the following way:

$$\begin{aligned} K_f(\tau) &= 2\gamma\delta(\tau) \\ K_s(\tau) &= ae^{-\lambda\tau} \end{aligned} \quad (9)$$

where γ is the damping rate due to the fast motion, λ^{-1} is the memory time of the slow motion, and a is its amplitude. Substituting the exact expression

$$\langle \Delta r^2(t) \rangle = 2\langle v^2 \rangle \int_0^t d\tau (t - \tau) C(\tau) \quad (10)$$

one can solve the differential equation and obtain an expression for the root-mean-square displacement in terms of a , γ , and λ . The mean square displacement is

$$\langle \Delta r^2(t) \rangle = 2\langle v^2 \rangle \int_C ds e^{st} \frac{(s + \lambda)}{s^2(s^2 + (\gamma + \lambda)s + \gamma\lambda + a)} \quad (11)$$

where s is the Laplace variable and C denotes the Bromwich contour. Solving for the zeros of the denominator, followed by use of the Cauchy residue theorem, gives $\langle \Delta r^2(t) \rangle$ in terms of the parameters (γ , λ , a).

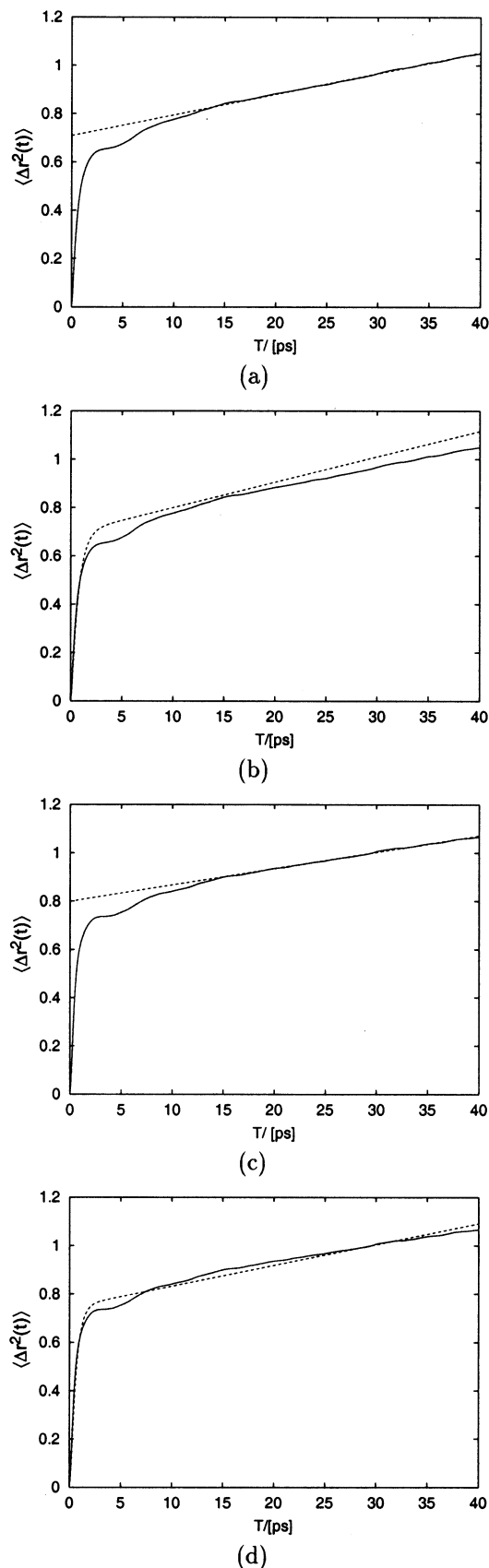


Figure 2. Parts a and c showing the average mean square displacement for [b mim] and [PF₆], respectively. Overlaid in the plots is the best straight-line fit to the linear part of the graph. From the linear fits, we computed corresponding self-diffusion coefficients for each of the ions using the Einstein relation $2Dt = 13\langle |r_i(t) - r_i(0)|^2 \rangle$. Parts b and d showing a comparison between the mean square displacement obtained from molecular dynamics simulations and that computed from a simple generalized Langevin model for [b mim] and [PF₆], respectively.

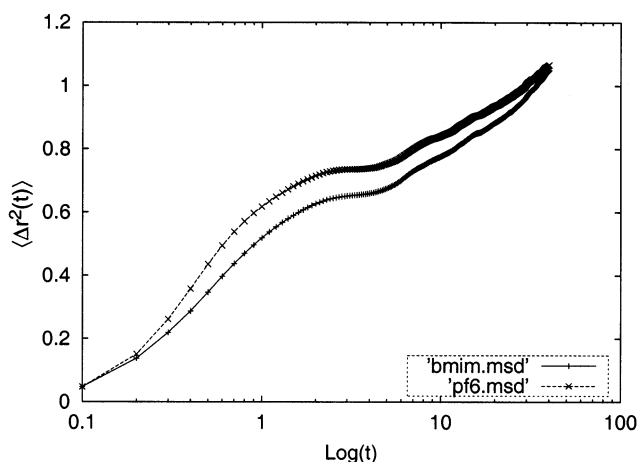


Figure 3. Average mean square displacement for [b mim] and [PF₆] as a function of the logarithm of time.

TABLE 1: Values of Parameters in the Generalized Langevin Model

parameters [ps ⁻¹]	[PF ₆]	[b mim]
λ	1.15×10^{-2}	1.5×10^{-2}
a	13.7788	15.3185
γ	8.7582	11.6265

Figure 2, parts b and d, display a comparison between the molecular dynamics results for the mean-square displacement and a fit of the Langevin model for [b mim] and [PF₆], respectively. The parameters a , γ , and λ are shown in Table 1. As can be appreciated in Figure 2 parts b and d, the model describes the dynamics reasonably well, but because of its simplicity, the intermediate region related to basin hopping is not described as well as other regions. Agreement could most likely be improved by choosing a more complicated functional form for the kernel and by introducing mode coupling theory.

If one compares the behavior of [b mim][PF₆] with that of liquid water at room temperature,²⁴ one can appreciate the fact that ionic liquids are “slow”, as is obvious from the fact that the diffusion constant is about 2 orders of magnitude smaller than that of water at the same temperature.

A crude upper bound estimate for the molar conductivity of the system can be obtained from the Nernst–Einstein equation:³

$$\Lambda_{N-E} = \frac{N_A e^2}{k_B T} (D_{[b\text{mim}]} + D_{[PF_6]}) \quad (12)$$

where N_A is Avogadro’s number and e is the electron charge. This equation assumes no ionic association and is derived for activity of the ions equal to unity. If we use this formula, we obtain a molar conductivity $\Lambda_{N-E} = 9.45 \times 10^{-5}$ S m²/mol, which corresponds to a conductivity $\kappa_{N-E} = 4.36 \times 10^{-1}$ S/m. Noda³ and co-workers measured diffusion coefficients and conductivities independently for similar compounds. They observed that the ratio between the measured molar conductivity and that computed using the diffusion coefficients of the ions assuming the Nernst–Einstein relation lies in the range $0.3 < \Lambda_{\text{Exp}}/\Lambda_{N-E} < 0.8$. This is due to the fact that the ions are associated, rather than moving completely independently. Suarez et al.¹⁰ measured $\kappa = 1.46 \times 10^{-1}$ S/m for [b mim][PF₆] at a temperature equal to 298.5 K. Because κ and Λ are simply related by the molar density, the ratio $\kappa_{\text{Exp}}/\kappa_{N-E}$ should satisfy the same relation. Taking the value of Suarez for κ_{Exp} and the value computed from our simulations for κ_{N-E} , we find $\kappa_{\text{Exp}}/$

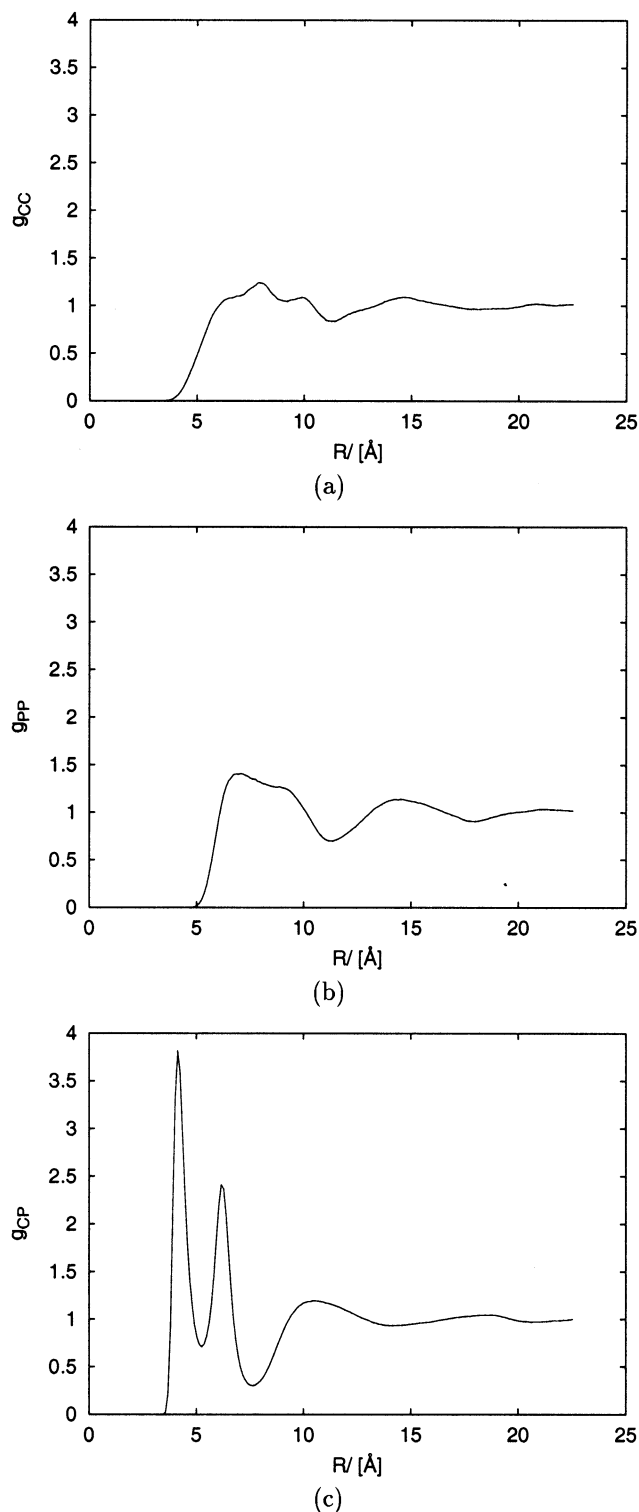


Figure 4. Parts a–c showing corresponding radial distribution functions for atoms C_1-C_1 , $P-P$, and C_1-P_1 , respectively.

$\kappa_{N-E} = 0.335$, indicating that our simulations are reasonably consistent with experimental conductivity measurements.

We also computed radial distribution functions for this system. In Figure 4a, $g_{CC}(r)$ corresponds to the radial distribution function for the carbon atom which lies between the two nitrogens of the imidazolium cation. Figure 4b, $g_{PP}(r)$, corresponds to the radial distribution function for the P atom in the hexafluorophosphate anion. Finally, in Figure 4c, we show $g_{CP}(r)$, the radial distribution function between aforementioned C and P atoms. It is clear that peaks in Figure 4c are sharper and larger than those in parts a and b of Figure 4 and appear at

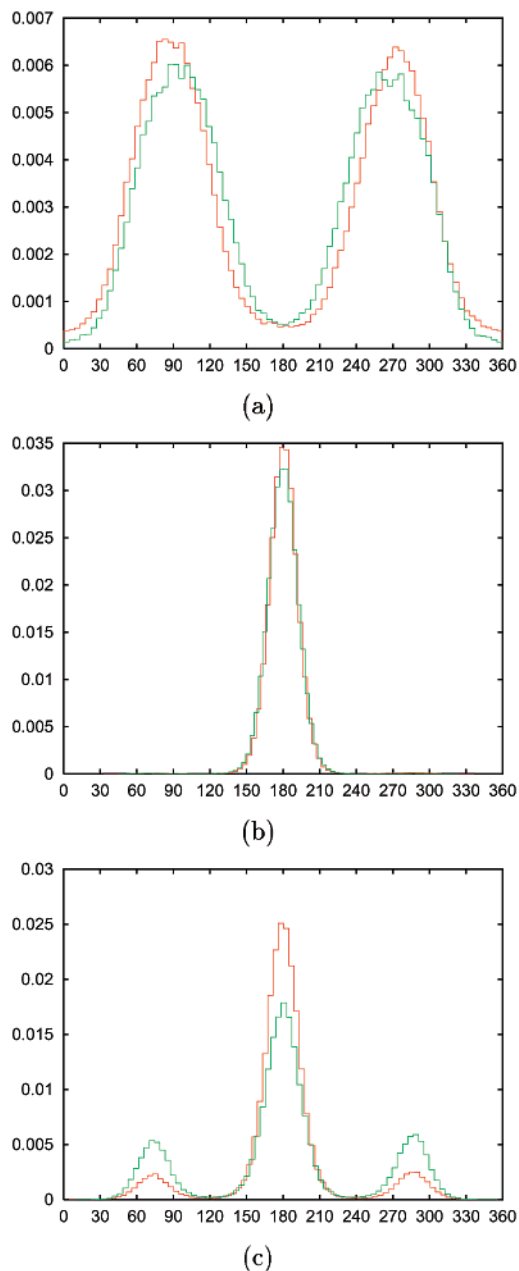


Figure 5. Parts a–c showing the equilibrium distribution functions for dihedral angles α_1 , α_2 , and α_3 defined in Figure 1 both in the liquid and for a single ion pair in the gas phase. (Liquid results are in red; ion pair results are in green).

shorter R . It is interesting to observe in all three radial distribution functions the fact that there seem to exist quite long spatial correlations. This is what one would expect from the strong Coulombic interactions between these molecules. Radial distribution functions in Figure 4 parts a and b appear less structured; peaks are wider and lower. However, the liquid structure seems to be persistent at distances larger than 20 Å.

Angular distribution functions for different dihedral angles defined in Figure 1 were computed both in the liquid and for an ionic pair in the gas phase. Results are displayed in Figure 5. It is clear from these plots that no major differences except in α_3 exist between the liquid and the gas phase.

4. Conclusions

In this paper, we studied transport and thermodynamic properties of a compound currently being developed both in

industry and academia as an alternative to volatile organic solvents. The dynamics of these liquids is slow and complex. Different time scales can be observed in the time history of the mean-square displacement of the center of mass of the ions. We believe the short-time behavior corresponds to the sampling of local basins, whereas the long-time behavior corresponds to diffusion. The characteristic initial quadratic dependence of the mean-square displacement indicating ballistic motion is observed only at very short times. Diffusion coefficients for each of the ions are in agreement with those found in the literature for similar organic ionic liquids. We computed them from the slope of the mean-square displacement using data in the range 20–40 ps in which the system appears to have reached the diffusional linear regime.

Using a simple model for the friction kernel in the generalized Langevin equation, we interpreted the results in terms of a slow and a fast process that one can associate with the sampling of a basin and a time-scale for escape and diffusion.

Several interesting questions remain for future analysis. Do all organic ionic liquids at room-temperature behave like cold liquids? What is the mechanism of solvation of polar and nonpolar molecules in them? We hope in the future to provide some answers to these questions. From the theoretical and computational point of view, free energies of solvation of different organic and inorganic molecules should be computed; partition coefficients and other similar properties would be useful as well. The calculation of radial and angular distribution functions for solutes in these liquids could shed light on possible mechanisms of solvation and perhaps reaction strategies. We plan in the future to pursue some of these calculations.

Acknowledgment. We would like to thank the Boston University Supercomputer Center for a generous allocation of computer time. This work was funded by the NSF grant CHE-00-76279.

Supporting Information Available: Table of all parameters used. This material is available free of charge via the Internet at <http://pubs.acs.org>.

References and Notes

(1) Welton, T. *Chem. Rev.* **1999**, *99*, 2071.

- (2) Holbrey, J. D.; Seddon, K. R. *J. Chem. Soc., Dalton Trans.* **1999**, *12*, 2133.
- (3) Noda, A.; Hayamizu, K.; Watanabe, M. *J. Phys. Chem. B* **2001**, *105*, 4603.
- (4) Wilkes, J. S.; Zaworotko, M. J. *J. Chem. Soc., Chem. Commun.* **1992**, *13*, 965.
- (5) Fuller, J.; Carlin, R. T.; Long, H. C. D.; Haworth, D. *J. Chem. Soc., Chem. Commun.* **1994**, *3*, 299.
- (6) Koel, M. *Proc. Est. Acad. Sci. Chem.* **2000**, *49*(3), 145.
- (7) Aki, S. N. V. K.; Brennecke, J. F.; Samanta, A. *Chem. Commun.* **2001**, *5*, 413.
- (8) Ngo, H. L.; LeCompte, K.; Hargens, L.; McEwen, A. B. *Thermochem. Acta* **2000**, *357–358*, 97.
- (9) Hagiwara, R.; Ito, Y. *J. Fluorine Chem.* **2000**, *105*, 221.
- (10) Suarez, P. A. Z.; Einloft, S.; Dullius, J. E. L.; de Souza, R. F.; Dupont, J. *J. Chim. Phys. Phys. Chim. Biol.* **1998**, *95*(7), 1626.
- (11) Hanke, C. G.; Price, S. L.; Lynden-Bell, R. M. *Mol. Phys.* **2001**, *99*, 801.
- (12) Hanke, C. G.; Atamas, N. A.; Lynden-Bell, R. M. *Green Chem.* **2002**, *4*(2), 107.
- (13) Lynden-Bell, R. M.; Atamas, N. A.; Vasilyuk, A.; Hanke, C. G. *Mol. Phys.* In press.
- (14) Jorgensen, W. L.; Maxwell, D. S.; Tirado-Rives, J. *J. Am. Chem. Soc.* **1996**, *118*, 11225.
- (15) Jaguar 4.1, Schrödinger, Inc.: Portland, OR, 1991–2000.
- (16) Kaminski, G. A.; Jorgensen, W. L. *J. Chem. Soc., Perkin Trans.* **1999**, *2*, 2365.
- (17) Zhou, R.; Harder, E.; Xu, H.; Berne, B. J. *J. Chem. Phys.* **2001**, *115*, 2348–2358.
- (18) Luty, B. A.; Tironi, I. G.; van Gunsteren, W. F. *J. Chem. Phys.* **1995**, *103*(8), 3014–3021.
- (19) Tuckerman, M.; Berne, B. J.; Martyna, G. J. *J. Chem. Phys.* **1992**, *97*, 1990.
- (20) Stuart, S. J.; Zhou, R.; Berne, B. J. *J. Chem. Phys.* **1996**, *105*, 1426.
- (21) Martyna, G. J.; Klein, M. L.; Tuckerman, M. E. *J. Chem. Phys.* **1992**, *97*, 2635.
- (22) Martyna, G. J.; Tobias, D. J.; Klein, M. L. *J. Chem. Phys.* **1994**, *101*, 4177.
- (23) Stern, H.; Xu, H.; Harder, E.; Rittner, F.; Pavese, M.; Berne, B. J. *SIM molecular dynamics simulation program*.
- (24) Stern, H.; Rittner, F.; Berne, B. J.; Friesner, R. A. *J. Chem. Phys.* **2001**, *115*, 2237.
- (25) Koishi, T.; Shirakawa, Y.; Tamaki, S. *J. Phys.: Condens. Matter* **1997**, *9*, 10101.
- (26) Gallo, P.; Sciortino, F.; Tartaglia, P.; Chen, S. H. *Phys. Rev. Lett.* **1996**, *76*, 2730.
- (27) Kurobori, T.; Yoshiura, M.; Liu, M.; Hirose, Y. *Jpn. J. Appl. Phys.* **1999**, *38*, 948.
- (28) Berne, B. J. Time correlation functions in condensed media. In *Physical Chemistry an advanced treatise*; Eyring, H.; Henderson, D.; Jost, W., Eds.; Academic Press: New York, 1971; Volume VIII B.